

Biotinylated Biodegradable Nanotemplated Hydrogel Networks for Cell Interactive Applications

Jason D. Clapper,[†] Megan E. Pearce,[‡] C. Allan Guymon,[†] and Aliasger K. Salem^{*,†,‡}

Department of Chemical and Biochemical Engineering, College of Engineering, and Division of Pharmaceutics, College of Pharmacy, University of Iowa, Iowa City, Iowa 52242

Received October 23, 2007; Revised Manuscript Received January 22, 2008

We describe the synthesis of a novel biotinylated nanotextured degradable hydrogel that can be rapidly surface engineered with a diverse range of biotinylated moieties. The hydrogel is synthesized by reacting methacrylated biotin-PEG with dimethacrylated PLA-*b*-PEG-*b*-PLA (LPLDMA, PEG = poly(ethylene glycol), PLA = poly(lactic acid)), or dimethacrylated PEG-*b*-PLA-*b*-PEG (PLPDMA). Methacrylated biotin-PEG is prepared by reacting biotin-PEG-OH with methacrylic anhydride. Biotin-PEG-OH is prepared by reacting α -hydroxy- ω -amine PEG with *N*-hydroxysuccinimide-biotin. Confirmation of the final product is determined using ¹H NMR and Fourier transform infrared spectroscopy (FTIR). The integrity and surface presentation of the biotin units is observed spectrophotometrically using the HABA/avidin assay. To produce nanostructured polymer topography, a self-assembling lyotropic liquid crystalline mesophase is used as a polymerization template, generating biotinylated hydrogels with highly organized lamellar matrix geometry. Traditionally processed isotropic hydrogels are used for comparison. Scanning electron microscopy shows that isotropic hydrogels have a smooth glassy appearance while lamellar templated hydrogels have defined surface topographical features that enhance preosteoblast human palatal mesenchymal cell (HEPM) attachment. Engineering the surfaces of the hydrogels with cell adhesive Arg-Gly-Asp (RGD) peptide sequences using the biotin-avidin interaction significantly enhances cell attachment. Surface engineering of cell adhesive peptides in conjunction with the lamellar template induced surface topography generates additive enhancements in cell attachment.

Introduction

Photopolymerized hydrogels have shown significant potential in a wide variety of applications ranging from scaffolds used in tissue engineering to prevention of thrombosis or biocompatible coatings.^{1–4} Hydrogels produced by photopolymerization are ideal for use as tissue engineering scaffolds because they can be polymerized in situ using minimally invasive strategies.^{5,6} Careful control over cross-linking density and the high water content of photopolymerized scaffolds allow for optimized mechanical properties and diffusion of desirable nutrients, oxygen, and other water soluble factors.⁷ The ideal photopolymerized scaffold should be degradable allowing for tailored drug or growth factor release.^{3,8} Such scaffolds should also be cell interactive allowing for optimal cell adhesion while seeding the scaffolds in vitro or promoting cell migration and adhesion in vivo.⁹ We have recently described a biodegradable photopolymerized hydrogel in which physical properties such as porosity, mechanical strength, and degradation can be carefully controlled on the nanoscale using lyotropic liquid crystals (LLCs) as photopolymerization templates.¹⁰

LLCs have been the focus of recent research due to their potential to generate nanostructured polymeric materials. LLC morphologies are created through the use of amphiphilic molecules that self-assemble into a number of nanostructured geometries depending on the size, shape, and chemical interaction of the surfactant molecule.¹¹ The highly organized arrangement of nanoscale order inherent in LLC morphologies have

been investigated as platforms for controlled chemical synthesis, compatibilization of immiscible polymer blends, and as templates to generate advanced polymeric structures.¹² Specifically, the use of various LLC geometries as polymerization templates directs the rate and conversion of templated polymerizations and controls the ultimate morphology, molecular weight, porosity, surface area, and physical properties of templated polymers.^{11–16}

We have recently shown that LLC templates may be used to structure-photopolymerizable biodegradable PLA-*b*-PEG-*b*-PLA (PEG = poly(ethylene glycol), PLA = poly(lactic acid)), resulting in bulk nanoscale lamellar morphology within the biopolymeric network.¹⁰ The ordering of the biodegradable monomer within the liquid crystal assembly increases both the rate and conversion of the polymerization reaction, minimizing unreacted monomer in the network, which is desirable for increased biocompatibility and increased mechanical strength. Creating a defined nanoscale network structure in photopolymerized PLA-*b*-PEG-*b*-PLA materials also yields an 80% increase in network swelling and an approximate 230% increase in diffusivity for large molecules.¹⁰ For example, rhodamine B isothiocyanate-dextran (MW 10000) is released in the LLC templated hydrogels at double the rate of release from isotropic hydrogels of the same monomer and composition.¹⁰ Control over the porosity and diffusivity in nanostructured, LLC templated hydrogels is essential for controlling the rate of release of larger therapeutic growth factors that may prove advantageous in future tissue engineering applications. Furthermore, control over the physical properties using LLC templating is very promising in the generation of highly advanced tissue scaffolds with precisely tuned properties.

* To whom correspondence should be addressed. E-mail: aliasger-salem@uiowa.edu.

[†] Department of Chemical and Biochemical Engineering, College of Engineering, University of Iowa.

[‡] Division of Pharmaceutics, College of Pharmacy, University of Iowa.

A critical parameter of this nanostructured degradable hydrogel that must be optimized for potential applications as a biomaterial or scaffold is the cell interactivity. Cell interactivity with biomaterials or scaffolds can be enhanced by surface engineering biomaterials with nano and micrometer scale topography or cell adhesive chemical cues.^{17–22} LLC templating may change the smooth surface associated with isotropic hydrogels to provide a textured surface that may result in increased cell adhesion. Additionally, an established approach to engineering cell adhesion consisting of incorporating amino acid sequences such as Arg-Gly-Asp (RGD) on the surface of biomaterials can be employed.^{4,5,23–25} The RGD cell adhesion peptide sequence is derived from extracellular matrices (ECM) such as fibronectin, vitronectin, and laminin.^{25,26} Using the smaller RGD peptide for surface modification instead of larger molecular weight ECM proteins is advantageous because the ECM protein can be randomly adsorbed to the surface so that the cell adhesive peptide sequences are not always exposed to the surface.²⁵ The smaller RGD peptide sequence is also more stable than ECM proteins and always exposed for cell binding. RGD/peptides are often attached to hydrogels through covalent linkage. For example, peptides can be incorporated into the bulk hydrogel during photopolymerization²² or free unreacted acrylate groups in the PEG networks can be used to chemically conjugate biological moieties.²⁷ However, the use of chemical reagents and solvents used for chemical conjugation can damage proteins and peptides that are easily susceptible to inactivation or denaturation.

In this study, we show that incorporating PEG-biotin into the degradable photopolymerized network generates a hydrogel that can be readily surface engineered with cell adhesive peptides under mild aqueous conditions. The PEG acts as a flexible spacer group for the biotin which reduces steric hindrance and therefore improves biotin binding to avidin.²⁸ Each biotin moiety presented by the hydrogel attaches to one of four biotin binding sites on the tetrameric protein avidin.²⁹ Two of the biotin binding pockets are located on the opposite side of the other two biotin binding pockets, which ensures that any bound avidin has available pockets to bind biotinylated peptide sequences or ligands. Furthermore, we show that biotinylated nanotextured photopolymers can be readily synthesized and surface engineered with RGD sequences for significantly enhanced cell attachment.

Experimental Section

Materials. Poly(ethylene glycol) (PEG, MW 2000), poly(ethylene glycol) monomethacrylate (PEGMA, MW 525), and hexamethylene diisocyanate (HMDI, MW 169) were obtained from Aldrich and dried prior to use via azeotropic distillation. DL-lactide was obtained from Polysciences and recrystallized in hexanes from ethyl acetate before use. Methacryloyl chloride, methacrylic anhydride, and stannous octanoate were obtained from Aldrich and used as received. The surfactant used to obtain nanotemplated surfaces was polyoxyethylene (10) cetyl ether (Brij 56, Aldrich). 1-Hydroxy-cyclohexyl phenyl-ketone (Irgacure 184, Ciba Specialty Chemicals) was used as the photoinitiator. α -Hydroxy- ω -amine PEG (MW 3400) and methoxy-terminated PEG (Mw 3000) were purchased from Nektar and dried prior to use via azeotropic distillation. Avidin (glycoprotein MW 66 kDa) was purchased from Sigma/Aldrich. Fluorescein isothiocyanate-biotin (FITC-biotin) was purchased from Molecular Probes. Biotin-(G₁₁)-GRGDS was custom synthesized by Sigma Genosys. *N*-Hydroxy succinimide (NHS) biotin was purchased from Pierce & Warriner. HABA (4'-hydroxyazobenzene-2-carboxylic acid)/avidin reagent was purchased from Sigma/Aldrich. Phalloidin-RITC was purchased from Molecular Probes. All solvents were purchased from Sigma/Aldrich.

Synthesis of Biotin-PEG-OH. α -Hydroxy- ω -amine PEG (1 g) was dissolved into acetonitrile (2 mL). Dichloromethane (DCM) (1 mL) and Et₃N (80 μ L) were added and the mixture then stirred for 1 min. After addition of NHS-biotin (0.250 g), the reactants were stirred overnight under argon. The slow addition of diethyl ether (40 mL) was used to precipitate the polymer, which was then filtered on a Buchner funnel and washed with diethyl ether. The isolated material was then dissolved in hot 2-propanol (70 °C) to give an opaque-cloudy solution. The polymer was reprecipitated on cooling; this product was then analyzed for biotin attachment by ¹H NMR spectroscopy. ¹H NMR spectra were recorded on a Bruker WM-360 spectrometer. ¹H NMR chemical shifts were measured in parts per million (ppm) relative to CHCl₃ in CDCl₃ and DMSO in DMSO-*d*₆. To remove water impurities and aqueous impurities from Biotin-PEG-OH, the polymer (350 mg) was dissolved into toluene (70 mL) and refluxed with a Dean-Stark trap and a condenser. Then 70% of the toluene was removed by distillation. The polymer was isolated on a rotary evaporator. To remove residual solvent, the polymer was dried under vacuum for 2 days. This experiment was repeated multiple times to generate sufficient quantities of biotin-PEG-OH.

Synthesis of Methacrylated PEG-Biotin and Methacrylated Methyl PEG. First, 0.04 g of biotin-PEG-OH (MW ~3600) was reacted with 0.3 mL of methacrylic anhydride in a 4 mL screw top vial with a stirrer bar at 60 °C for 24 h. The reaction mixture was cooled and then added to 3 mL of ethyl ether to precipitate the biotin-PEG-MA product. The product was centrifuged, the liquid was decanted, and the product dried overnight in a vacuum oven. The product was dissolved in 0.2 mL of DCM, precipitated in 3 mL of ethyl ether, decanted, and dried again. The resulting product mass was 0.03 g. Confirmation of successful methacrylation was provided by Fourier transform infrared (FTIR) spectroscopy (Thermo Electron Nexus 670). The FTIR was purged with nitrogen to reduce noise from water vapor and carbon dioxide. Samples containing 15 μ m glass spacers were sandwiched between two NaCl slides (International Crystal Laboratories). At least 64 spectra were collected at 8 cm⁻¹ resolution and averaged for final analysis. The same synthesis steps were followed for the methyl-PEG-OH synthesis using a methyl-PEG-OH (MW 3000).

Synthesis of PLA-PEG-PLA-dimethylacrylate and PEG-PLA-PEG-dimethylacrylate. The biodegradable polymeric materials prepared for this study include PLA-PEG-PLA dimethylacrylate (LPLDMA) with a 2000 molecular weight central PEG chain, 4 lactide groups on each end of the PEG block, and methacrylate terminal groups. Briefly, PEG was reacted with DL-lactide using stannous octanoate as a catalyst for the ring opening addition of PLA onto the central PEG chain. Methacrylate groups were then added to PEG-PLA product using methacryloyl chloride and previously defined synthesis methods.³ The second biodegradable polymer platform used was PEG(2000)-PLA-PEG(2000) dimethylacrylate (PLPDMA) synthesized with a 5:1 ratio of ethylene glycol (EG) to lactide (LA) groups and dimethylacrylate functionality.¹⁰ Briefly, a 1:1 molar ratio of PEGMA and DL-lactide was dissolved in toluene at reflux conditions (115 °C) for 12 h using stannous octanoate as the ring opening catalyst. The vessel was cooled to 60 °C and HMDI was added using a 1:0.5 molar ratio of PEGMA to HMDI to couple the PEGMA-PLA chains.

Synthesis of Biotinylated Hydrogels. Both LPLDMA and PLPDMA biomaterials were fabricated in an isotropic state using 40 wt % macromer in water with 0.75 wt % I-184 photoinitiator as well as in a nanostructured lamellar LLC template using 40 wt % macromer, 45 wt % Brij 56 surfactant, water, and 0.75 wt % I-184 photoinitiator. In the surface modified cases, 4 wt % of the total macromer loading in the LPLDMA formulations and 7.5 wt % of the total macromer loading in the PLPDMA formulations were replaced with the methacrylated PEG-Biotin. Sample formulations were mixed thoroughly at 55 °C for 4 h in a small vial. Hydrogel squares were fabricated by pouring 1 mL of the monomer solutions described above into a nylon mold with 2 cm \times 2 cm \times 0.25 cm troughs. The mold was placed in a nitrogen purged box for 10 min and then irradiated using a 365 nm UV light

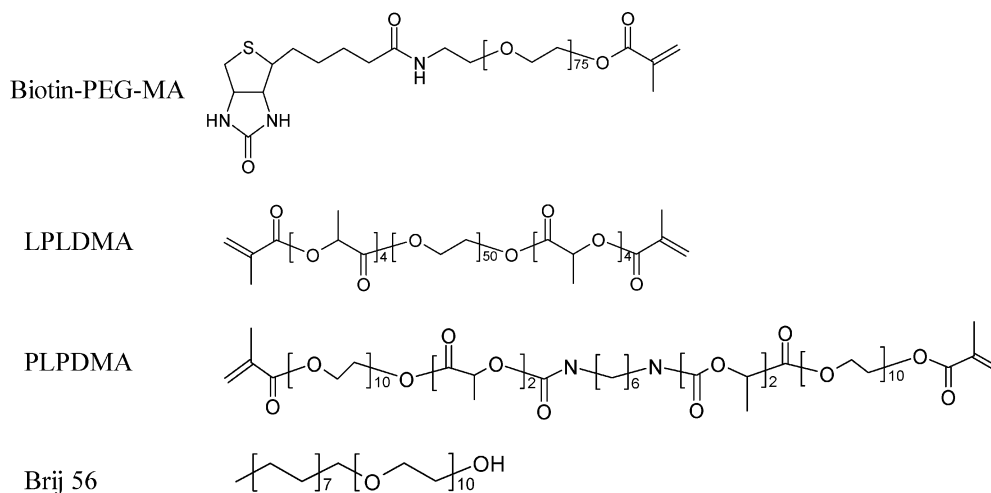


Figure 1. Structures of Biotin-PEG-MA, LPLDMA, PLPDMA, and Brij 56.

source (1.8 mW/cm², 10 min). For physical property analysis, disks were punched from these square hydrogel samples for both swelling and modulus tests. For cell attachment analysis, 5 mm × 5 mm × 3 mm squares were cut from the bulk samples. All samples were soaked in an ethanol solution for 24 h to remove the surfactant and unreacted monomer, and then dried overnight in a vacuum oven.

Physical Property Analysis. Water uptake was measured gravimetrically by placing the dried hydrogel disks into 37 °C phosphate buffered saline (PBS, 0.15 M) solution (pH 7.4). Swelling measurements were taken by removing a disk from solution, patting the surface dry, and recording the mass of the sample. Initial equilibrium water uptake was determined once the mass of the hydrated sample did not change significantly as a function of overall swell time (approximately 3–5 h) and was calculated using previously defined methods.¹⁴ Although these materials are degradable in water, the 3–5 h time frame to reach the swelling pseudoequilibrium is much shorter than the typical degradation times for these platforms of 2–3 months. Thus, by performing the swelling and mechanical tests within a few days of rehydration, these properties are not expected to be influenced by degradative mechanisms. Dynamic mechanical analysis (DMA, TA instruments Q800 series) was used to determine the compressive modulus of the swollen hydrogel disks. Hydrogels were incubated in 37 °C PBS for 24 h prior to the compressive test. Disk shaped samples were placed on the compressive clamp of the DMA and compressed to approximately 90–95% of their original height. Compressive modulus was determined using the stress/strain curves from the DMA results. In both the swelling and modulus tests, three samples of each test material were analyzed to obtain a standard deviation for each resulting data point.

Absorbance Spectroscopy Studies Using the [2-(4'-Hydroxy-azobenzene)benzoic acid] (HABA)/Avidin Reagent. Spectroscopy studies were completed on a SPECTRAMax PLUS (Molecular Devices) at a fixed wavelength of 500 nm at 37 °C. The average read time was 0.5 s. Three blanks were read followed by three readings of the HABA/avidin in 1 mL cuvettes. Each sample was recorded three times over a subset of four repeats. The assay was completed by measuring the absorbance of the avidin-HABA complex at 500 nm before and after (10 min) it had been placed over the biotin presenting hydrogel substrate. The absorption decreases proportionately to the biotin present on the surface because biotin displaces HABA due to its higher affinity for avidin. The change in absorbance can then be used to calculate the amount of biotin present. A series of biotin solutions of varying concentration were prepared as a calibration curve for determining the quantity of biotin molecules present on the surface of the hydrogel.

Scanning Electron Microscopy. Surface morphology was assessed by scanning electron microscopy (SEM, Hitachi S-4000). Briefly, air-dried hydrogel samples were placed on adhesive carbon tabs mounted on SEM specimen stubs. The specimen stubs were coated with

approximately 5 nm of gold by ion beam evaporation before examination in the SEM operated at 5 kV accelerating voltage.

Surface Functionalization of Polymer Substrates with RGD Peptides. A 500 µg/mL solution of avidin was prepared using distilled water. The avidin solution was pipetted onto the biotinylated polymer surface until it was completely covered. After 1 h, the avidin solution was removed and replaced with an excess of distilled water. After 5 min, the water was removed. This washing procedure was repeated five times. The biotinylated peptide sequences were sterilized under UV light for 15 min. A 1 mg/mL solution of peptide was incubated over the avidinylated polymer samples and allowed to incubate at 37 °C on a shaker plate for 20 min. The samples were washed three times with sterile PBS prior to seeding with cells.

Cell Attachment Assay. Preosteoblast human palatal mesenchymal cells (HEPM 1486; ATCC, Manassas, VA) were grown to confluence in Eagle's minimum essential medium (EMEM) supplemented with Earle's salts, L-glutamine (2 mM), nonessential amino acids (0.1 mM), sodium pyruvate (1 mM), 10% fetal bovine serum, and 25 µg/mL penicillin-streptomycin. They were then plated onto the sterilized hydrogel samples in the same culture medium at a seeding density of 1 × 10⁶ cells. Cultures were allowed to attach for 1 h before replacing with 1 mL of media. After 2 additional hours, the media was removed from the wells. Immunofluorescent analysis was performed by fixing cells in 3.7% paraformaldehyde in PBS for 10 min. The cells were then rinsed in 1 × PBS followed by permeabilization for 8 min in 0.5% Triton X-100 in PBS. Following rinsing with 1 × PBS, cells were stained with phalloidin-RITC (1:500) for 45 min at 37 °C, after which the samples were washed in 1 × PBS for 5 min, rinsed in deionized water for 1 min, and mounted with Fluoromount (Sigma). The samples were viewed on an Olympus CKX41 (Leeds Precision Instruments, Minneapolis, MN) microscope equipped with epifluorescence optics and a 10× objective (total magnification 100×). Measurement of cell attachment was carried out by inverting the samples and counting absolute cell numbers, *n* = 3 per condition. Values were normalized to a percent cell attachment on tissue culture plastic.

Statistical Analysis. Group data were reported as mean ± SD. Differences between groups were analyzed by one way analysis of variance with a Tukey post-test analysis. Levels of significance were accepted at the *P* < 0.05 level. Statistical analyses were performed using Prism 3.02 software (Graphpad Software, Inc., San Diego, CA.).

Results and Discussion

Synthesis of biotinylated nanotextured hydrogels requires three core components: biotin-PEG-MA, LPLDMA or PLPDMA, an aqueous solution of Brij 56 (Figure 1). The LPLDMA and PLPDMA monomers form the main backbone of the

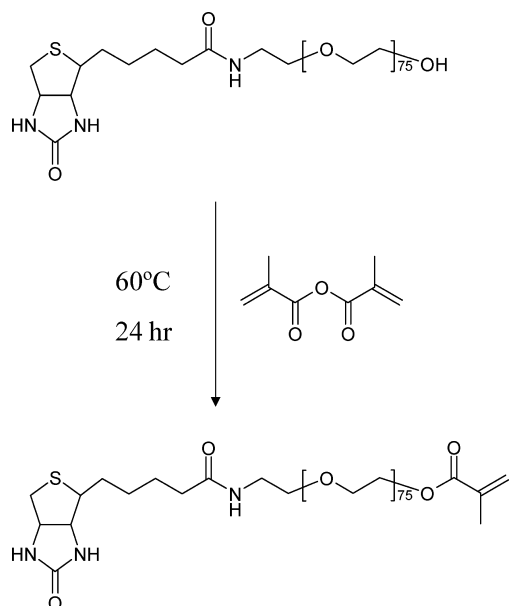


Figure 2. Synthesis of Biotin-PEG-MA.

hydrogel and contain the degradable lactic acid units. Brij 56 self-assembles in water to form the lamellar lyotropic liquid crystal (LLC) geometry that serves to direct the structure of the forming biopolymer into the desired morphology. The biotin-PEG-MA homogeneously incorporates the biotin group throughout the hydrogel network. The PEG unit attached to the biotin is critical for surface presentation of biotin without steric hindrance and for ensuring receptor mediated specific binding of avidin.²² Biotin-PEG-MA was prepared by first synthesizing Biotin-PEG-OH. Biotin-PEG-OH was prepared by attaching biotin to the α -hydroxy- ω -amine PEG using *N*-hydroxy-succinimide chemistry. ¹H NMR spectra of HO-PEG-biotin show the appearance of a triplet at 2.05 ppm due to the methylene from the biotin chain next to the amide and a broad singlet assigned to the free amido proton at 7.85 ppm. These signals do not appear on control ¹H NMR spectra of NHS-biotin. Two methine protons (H-3, H-4) from the cyclic biotin structure at 4.3 and 4.2 ppm and two urea protons (H-1', H-3') from the cyclic biotin structure at 6.45, 6.35 ppm identify the biotin group. Once the biotin-PEG-OH was synthesized, it was reacted with methacrylic anhydride to produce biotin-PEG-MA (Figure 2). Confirmation of the product was observed by the disappearance of the broad hydroxyl peak at 3300–3600 cm^{-1} and the appearance of the methacrylate double bond peak at 814 cm^{-1} in FTIR spectra. Next, we synthesized the LPLDMA and the PLPDMA. ¹H NMR and IR confirmed that PLA had attached onto the central PEG group with NMR peaks at 1.5, 4.2, and 5.2 ppm and the expansion of an IR peak at 1750 cm^{-1} . Confirmation of vinyl group addition to the macromer was seen through the presence of ¹H NMR peaks at 5.8, 6.1 and 6.4 ppm and the appearance of FTIR peaks at 806 and 1640 cm^{-1} .

Figure 3 shows our general approach to synthesizing the biotinylated nanotextured biodegradable hydrogel. Both LPLDMA and PLPDMA hydrogels were fabricated in an isotropic state using 40 wt % macromer in water with 0.75 wt % I-184 photoinitiator, as well as in a nanostructured lamellar LLC template using 40 wt % macromer, 45 wt % Brij 56 surfactant, water, and 0.75 wt % I-184 photoinitiator. Although the binary system of Brij 56 and water exhibits numerous LLC morphologies including normal hexagonal, normal bicontinuous cubic, and lamellar phases,¹¹ only the lamellar and hexagonal phases are observed when the biodegradable macromers are incorpo-

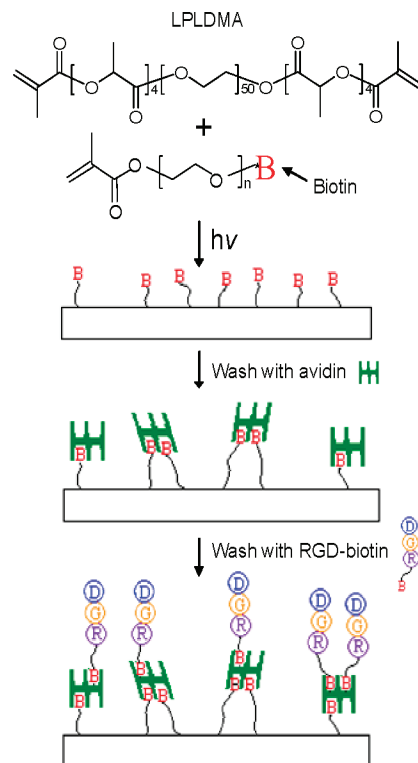


Figure 3. Synthesis of RDG-modified nanotextured hydrogels through the biotin-avidin surface engineering approach.

rated into the formulations.¹⁰ The large hydrophilic LPLDMA macromer specifically limits the formation of the curved geometries of the hexagonal and cubic phases, leaving the lamellar phase as the most entropically favored morphology.¹⁰ In the current study, the lamellar phase template was selected in the photopolymerization for both LPLDMA and PLPDMA due to the stability of this LLC mesophase even with the addition of the biotinylated PEGMA.

To confirm that modification of the hydrogel with biotinylated PEG moieties did not significantly affect the physical properties of the hydrogels, isotropic and templated LPLDMA were photopolymerized with 4% PEGMA, and isotropic and templated PLPDMA were photopolymerized with 7.5% PEGMA. In physical property analysis, the most significant differences in mechanical strength were observed between isotropic and lamellar hydrogels. For example, the compressive modulus of hydrogels prepared from LPLDMA reduced by approximately 2.5 fold when LPLDMA was prepared in the lamellar phase in comparison to the isotropic phase (Figure 4). Similar reductions in compressive modulus were observed for PLPDMA. Within either the isotropic or lamellar set, the addition of PEGMA associated with the methacrylated PEG-biotin does not significantly change the compressive modulus in degradable hydrogels prepared from LPLDMA or PLPDMA.

The mechanical property results are consistent with the percentage water uptake studies (Figure 5) performed in this study. Lamellar templated LPLDMA hydrogels demonstrated a 1.7 to 1.9 fold increase in water uptake in comparison to isotropic hydrogels. The greater swelling of the lamellar templated gel also serves to reduce compressive modulus in this system. Similarly, isotropic PLPDMA hydrogels also show a 1.3 to 1.5 fold lower water uptake than lamellar PLPDMA hydrogels. In addition to cross-linking, the chemical structure of the hydrogel is also a major factor in water uptake. For example, the isotropic PLPDMA hydrogels have a 1.4 fold lower

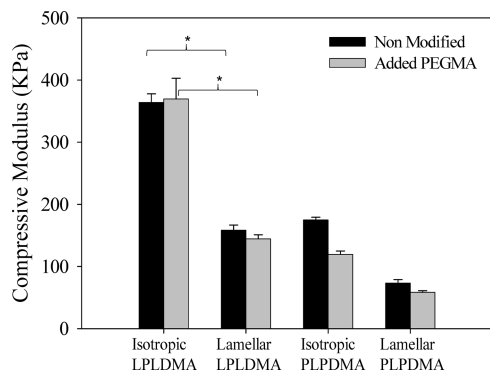


Figure 4. Graph showing compressive modulus of isotropic LPLDMA, lamellar LPLDMA, isotropic PLPDMA, and lamellar PLPDMA (with and without additional PEG-MA). Bars represent mean \pm standard deviation. * = significance at $P < 0.05$.

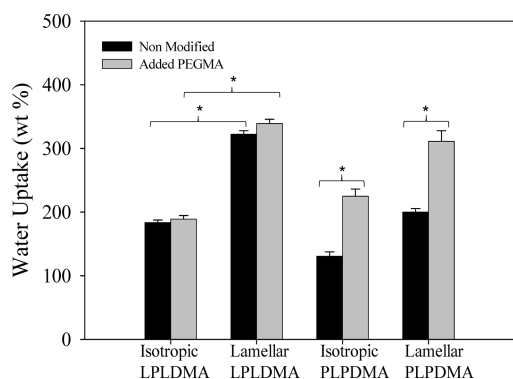


Figure 5. Graph showing percentage water uptake of isotropic LPLDMA, lamellar LPLDMA, isotropic PLPDMA, and lamellar PLPDMA. Bars represent mean \pm standard deviation. * = significance at $P < 0.05$.

water uptake than isotropic LPLDMA hydrogels which is associated with the higher hydrophobic PLA content of the PLPDMA gel. Correlating with the compressive modulus studies, the addition of 4% PEGMA does not significantly change the percentage water uptake in isotropic and lamellar LPLDMA hydrogels. However, addition of 7.5% PEGMA to the more hydrophobic PLPDMA system increases water uptake 1.6 to 1.7 fold in isotropic and lamellar templated hydrogels. It is reasonable to assume from these results that addition of the linear methacrylated biotin-PEG-MA will modify the physical properties in the isotropic and lamellar templated hydrogels in a concentration dependent manner by reducing the cross-linking density of the overall gel and increasing the hydrophilic components of the gel.

The smooth morphology of the LPLDMA hydrogel in an isotropic phase without added surfactant is shown in scanning electron micrographs in Figure 6A. The addition of methacrylated PEG-biotin does not change the surface morphology (Figure 6B). In contrast, LPLDMA hydrogels prepared with a lamellar Brij 56 template produce well-defined sheetlike morphologies as shown in Figure 6C. Defined grain boundaries appear in the hydrogel network suggesting that monomer diffusion is directed by the LLC phase. Features are 3–6 μm in length, 100–300 nm in width and separated by 500 nm to 2 μm spacings. This is consistent with our previous observations in LLC templated acrylamide photopolymerizations and the observations of Antonietti et al. who proposed that the domain growth is regulated by the anisotropic transport properties of the liquid crystalline phase.^{13,30} Similar observations were noted for the PLPDMA hydrogels.

Next, we quantified the number of biotin groups available for surface engineering with avidin. Absorbance spectroscopy studies using the HABA/avidin complex show that isotropic LPLDMA hydrogel samples had 1.54×10^{-17} mol PEG-biotin/ μm^2 . Isotropic PLPDMA hydrogel samples had 2.68×10^{-17} mol PEG-biotin/ μm^2 which is proportional with the amount of PEG-biotin added during polymerization. To confirm that biotinylated peptide sequences would bind to the surface via the avidin linker, we functionalized the surface of the biotin presenting LPLDMA with a biotinylated peptide sequence (biotin-(G₁₁)-GRDGS) that contains the cell adhesive peptide Arg-Gly Asp (RGD). RGD promotes cell attachment and spreading through cell surface integrin receptors. The sequence binds to many integrin receptors including $\alpha_5\beta_3$ and $\alpha_5\beta_1$.^{23–25,31,32} Spaced between the biotin unit and the RGD moiety, we included eleven glycines to provide adequate distance from the avidin binding pocket.³³ Receptor mediated specific binding of the biotin-(G₁₁)-GRDGS was confirmed using fluorescent binding studies in which avidin-immobilized LPLDMA-biotin samples were exposed to the biotin-(G₁₁)-GRDGS, washed, and then exposed to a solution of biotin-FITC and re-washed. No fluorescence was observed by fluorescence microscopy providing confirmation that all the biotin binding pockets are bound with biotin-(G₁₁)-GRDGS moieties. In control experiments, exposure of the hydrogel samples to biotin-FITC without prior exposure to the biotin-(G₁₁)-GRDGS generate high intensities of fluorescence.

Next, nine samples were prepared for cell attachment studies: isotropic PEG-MA, isotropic LPLDMA, isotropic LPLDMA with biotin-PEG-MA, lamellar LPLDMA, lamellar LPLDMA with biotin-PEG-MA, isotropic PLPDMA, isotropic PLPDMA with biotin-PEG-MA, lamellar PLPDMA and, lamellar PLPDMA with biotin-PEG-MA. Each group was incubated with avidin, washed and then incubated with biotin-(G₁₁)-GRDGS. Preosteoblast human palatal mesenchymal (HEPM) cells were selected for cell attachment studies because of their known integrin mediated interactions with the RGD peptide sequence.³⁴ Isotropic PLPDMA without biotin-PEG-MA shows a 3.5 fold higher cell attachment than isotropic LPLDMA without biotin-PEG-MA (Figure 7). This is presumably because the PLPDMA has a higher ratio of PLA to PEG, increasing its hydrophobicity and ability to adsorb ECM proteins that promote cell attachment. Isotropic PLPDMA with biotin-PEG-MA induces a 1.5 fold higher cell attachment than isotropic LPLDMA with biotin-PEG-MA because of increased hydrophobicity and because of a 1.75-fold increase in presentation of biotin groups as determined by the HABA/avidin assay. An increase in biotin presentation and therefore cell attachment is correlated with the increase in biotin-PEG-MA introduced into the polymerization. In future studies, it would be valuable to determine the biotin-PEG-MA concentration dependence on cell attachment. This lamellar LPLDMA without biotin-PEG-MA shows a 1.75 fold increase in cell attachment in comparison to isotropic LPLDMA without biotin-PEG-MA. Lamellar PLPDMA without biotin-PEG-MA induces a 1.2 fold increase in cell attachment in comparison to isotropic PLPDMA without biotin-PEG-MA. In both cases, the positive surface features (Figure 6C) associated with LLC lamellar templated photopolymerization provide enhanced cell attachment in comparison to the smooth surfaces associated with isotropic hydrogels. It has been hypothesized that surface features can increase hydrophobicity by trapping air molecules on the substrate, provide attachment points for extending filopodia to attach to and for cells to form focal adhesion points and provide enhanced

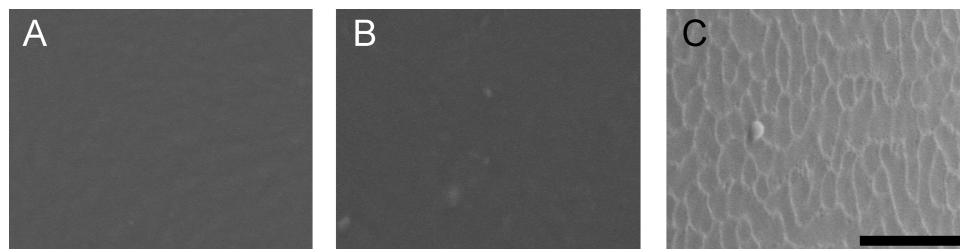


Figure 6. Scanning electron micrographs showing surface morphology of (a) isotropic LPLDMA, (b) isotropic LPLDMA with biotin-PEG-MA, and (c) lamellar LPLDMA with biotin-PEG-MA. Bar = 10 μm .

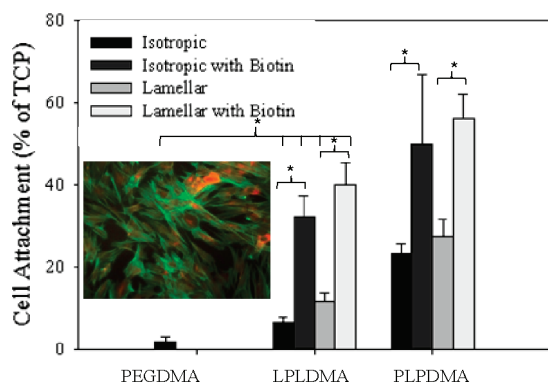


Figure 7. Graph showing percentage cell attachment (of tissue culture plastic (TCP)) on PEGDMA, isotropic LPLDMA, isotropic PLPDMA, lamellar LPLDMA, and lamellar PLPDMA (with and without biotin-PEG-MA) after incubation and washes with avidin and biotin-(G11)-GRGDS. Bars represent mean \pm standard deviation. * = significance at $P < 0.05$. Inserted in the figure is a fluorescent microscopy image showing cell morphology of HEPM cells attached to the isotropic PLPDMA with biotin-PEG-MA and after surface engineering with avidin and biotin-(G11)-GRGDS after 72 h.

adsorption of ECM proteins that then promote cell attachment.^{17,18,35–39} Isotropic LPLDMA with biotin-PEG-MA increases cell attachment by 4.85 fold in comparison to isotropic LPLDMA without biotin-PEG-MA. The presence of the biotin-PEG-MA in the hydrogel is critical for binding biotin-(G₁₁)-GRGDS, which in turn significantly enhances cell attachment via integrin specific receptor binding. Lamellar LPLDMA with biotin-PEG-MA generates a 1.24 fold increase in cell attachment in comparison to isotropic LPLDMA with biotin-PEG-MA suggesting that engineered topography and cell adhesion molecules can be used additively to enhance cell attachment in these novel biodegradable hydrogels. Figure 7 also shows that HEPM cells attached to the RGD surface engineered substrates were spreading well with healthy cytoskeletal structure and morphology by 72 h. Control hydrogel samples prepared from PEGDMA alone resulted in negligible cell attachment and cells attached to the substrate by 72 h had not spread well and were predominantly rounded and dying. This is consistent with previous observations from us and others that PEG significantly reduces cell attachment because of PEGs protein resistance properties.^{40–43}

Conclusions

Hydrogels that integrate cell interactivity into their surface properties are critical in the development of these materials in drug delivery and tissue engineering applications. In this study, we describe a novel biotinylated nanotemplated degradable hydrogel that can be rapidly surface engineered under mild aqueous conditions using the biotin-avidin interaction. The bulk properties of the hydrogel such as degradation, porosity,

mechanical strength and water uptake can be controlled by the incorporation of a nanoscale LLC template during the photopolymerization reaction, directing the growing polymer morphology. The identifiable surface features generated from the LLC templated polymerizations enhance cell attachment. Addition of methacrylated-PEG-biotin in the hydrogel polymerization provides a mechanism by which the surface of the hydrogel could be surface engineered with a wide variety of cell adhesive ligands in combination or alone. This approach has significant potential for bioassays, targeted drug delivery or for patterning of cells using microfluidic technology.

Acknowledgment. A. K. Salem acknowledges financial support through NSF NER (CMMI-0608977) and an American Cancer Society Junior Faculty award (IRG-77-004-28). C. A. Guymon acknowledges support from NSF grants (PECASE CBET-0328231 and CBET-0626395) and a Biosciences Initiative Pilot Grant from the University of Iowa. J. D. Clapper acknowledges support from a presidential fellowship from the University of Iowa.

References and Notes

- (1) Tessmar, J. K.; Gopferich, A. M. *Macromol. Biosci.* **2007**, *7* (1), 23–39.
- (2) Sharma, B.; Williams, C. G.; Khan, M.; Manson, P.; Elisseeff, J. H. *Plast. Reconstr. Surg.* **2007**, *119* (1), 112–120.
- (3) Sawhney, A. S.; Pathak, C. P.; Hubbell, J. A. *Macromolecules* **1993**, *26* (4), 581–587.
- (4) Peppas, N. A.; Hilt, J. Z.; Khademhosseini, A.; Langer, R. *Adv. Mater.* **2006**, *18* (11), 1345–1360.
- (5) Drury, J. L.; Mooney, D. J. *Biomaterials* **2003**, *24* (24), 4337–4351.
- (6) Baroli, B. *J. Chem. Technol. Biotechnol.* **2006**, *81* (4), 491–499.
- (7) Sheng, L. G.; Jones, R. L.; Washburn, N. R.; Horkay, F. *Macromolecules* **2005**, *38* (7), 2897–2902.
- (8) Salem, A. K.; Rose, F.; Oreffo, R. O. C.; Yang, X. B.; Davies, M. C.; Mitchell, J. R.; Roberts, C. J.; Stolnik-Trenkic, S.; Tendler, S. J. B.; Williams, P. M.; Shakesheff, K. M. *Adv. Mater.* **2003**, *15* (3), 210–213.
- (9) Martina, M.; Huttmacher, D. W. *Polym. Int.* **2007**, *56* (2), 145–157.
- (10) Clapper, J. D.; Iverson, S. L.; Guymon, C. A. *Biomacromolecules* **2007**, *8*, 2104–2111.
- (11) DePierro, M. A.; Guymon, C. A. *Macromolecules* **2006**, *39* (2), 617–626.
- (12) Clapper, J. D.; Guymon, C. A. *Macromolecules* **2007**, *40* (4), 1101–1107.
- (13) DePierro, M. A.; Carpenter, K. G.; Guymon, C. A. *Chem. Mater.* **2006**, *18* (23), 5609–5617.
- (14) Lester, C. L.; Smith, S. M.; Colson, C. D.; Guymon, C. A. *Chem. Mater.* **2003**, *15* (17), 3376–3384.
- (15) Lester, C. L.; Guymon, C. A. *Polymer* **2002**, *43* (13), 3707–3715.
- (16) Guymon, C. A.; Hoggan, E. N.; Clark, N. A.; Rieker, T. P.; Walba, D. M.; Bowman, C. N. *Science* **1997**, *275* (5296), 57–59.
- (17) Wong, J. Y.; Leach, J. B.; Brown, X. Q. *Surf. Sci.* **2004**, *570* (1–2), 119–133.
- (18) Webster, T. J.; Ergun, C.; Doremus, R. H.; Siegel, R. W.; Bizios, R. *Biomaterials* **2001**, *22* (11), 1327–1333.
- (19) Webster, T. J.; Ahn, E. S. Nanostructured biomaterials for tissue engineering bone. In *Tissue Engineering II: Basics of Tissue Engineer-*

- ing and Tissue Applications; Advances in Biochemical Engineering/ Biotechnology, Vol. 103; Springer: New York, 2007; pp 275–308.
- (20) Shakesheff, K. M.; Cannizzaro, S. M.; Langer, R. *J. Biomater. Sci., Polym. Ed.* **1998**, *9* (5), 507–518.
- (21) Salem, A. K.; Stevens, R.; Pearson, R. G.; Davies, M. C.; Tandler, S. J. B.; Roberts, C. J.; Williams, P. M.; Shakesheff, K. M. *J. Biomed. Mater. Res.* **2002**, *61* (2), 212–217.
- (22) Hern, D. L.; Hubbell, J. A. *J. Biomed. Mater. Res.* **1998**, *39* (2), 266–276.
- (23) Bini, E.; Foo, C. W. P.; Huang, J.; Karageorgiou, V.; Kitchel, B.; Kaplan, D. L. *Biomacromolecules* **2006**, *7* (11), 3139–3145.
- (24) Deng, C.; Tian, H. Y.; Zhang, P. B.; Sun, J.; Chen, X. S.; Jing, X. B. *Biomacromolecules* **2006**, *7* (2), 590–596.
- (25) Ruoslahti, E.; Pierschbacher, M. D. *Science* **1987**, *238* (4826), 491–497.
- (26) Lee, K. Y.; Alsberg, E.; Hsiong, S.; Comisar, W.; Linderman, J.; Ziff, R.; Mooney, D. *Nano Lett.* **2004**, *4* (8), 1501–1506.
- (27) Gobin, A. S.; West, J. L. *J. Biomed. Mater. Res., Part A* **2003**, *67* (1), 255–259.
- (28) Salem, A. K.; Cannizzaro, S. M.; Davies, M. C.; Tandler, S. J. B.; Roberts, C. J.; Williams, P. M.; Shakesheff, K. M. *Biomacromolecules* **2001**, *2* (2), 575–580.
- (29) Wilchek, M.; Bayer, E. A.; Livnah, O. *Immunol. Lett.* **2006**, *103* (1), 27–32.
- (30) Antonietti, M.; Caruso, R. A.; Goltner, C. G. *Macromolecules* **1999**, *32* (5), 1383–1389.
- (31) Irvine, D. J.; Ruzette, A. V. G.; Mayes, A. M.; Griffith, L. G. *Biomacromolecules* **2001**, *2* (2), 545–556.
- (32) DeLong, S. A.; Gobin, A. S.; West, J. L. *J. Controlled Release* **2005**, *109* (1–3), 139–148.
- (33) Cannizzaro, S. M.; Padera, R. F.; Langer, R.; Rogers, R. A.; Black, F. E.; Davies, M. C.; Tandler, S. J. B.; Shakesheff, K. M. *Biotechnol. Bioeng.* **1998**, *58* (5), 529–535.
- (34) Schneider, G. B.; English, A.; Abraham, M.; Zaharias, R.; Stanford, C.; Keller, J. *Biomaterials* **2004**, *25* (15), 3023–3028.
- (35) Kim, P.; Kim, D. H.; Kim, B.; Choi, S. K.; Lee, S. H.; Khademhosseini, A.; Langer, R.; Suh, K. Y. *Nanotechnology* **2005**, *16* (10), 2420–2426.
- (36) Milner, K. R.; Siedlecki, C. A. *J. Biomed. Mater. Res., Part A* **2007**, *82* (1), 80–91.
- (37) Ismail, F. S. M.; Rohanizadeh, R.; Atwa, S.; Mason, R. S.; Ruys, A. J.; Martin, P. J.; Bendavid, A. *J. Mater. Sci.: Mater. Med.* **2007**, *18* (5), 705–714.
- (38) Kunzler, T. P.; Drobek, T.; Schuler, M.; Spencer, N. D. *Biomaterials* **2007**, *28* (13), 2175–2182.
- (39) Hamilton, D. W.; Brunette, D. M. *Biomaterials* **2007**, *28* (10), 1806–1819.
- (40) Baman, N. K.; Schneider, G. B.; Terry, T. L.; Zaharias, R.; Salem, A. K. *Int. J. Nanomed.* **2006**, *1* (2), 213–217.
- (41) Sinclair, J.; Salem, A. K. *Biomaterials* **2006**, *27* (9), 2090–2094.
- (42) VandeVondele, S.; Voros, J.; Hubbell, J. A. *Biotechnol. Bioeng.* **2003**, *82* (7), 784–790.
- (43) Kingshott, P.; McArthur, S.; Thissen, H.; Castner, D. G.; Griesser, H. J. *Biomaterials* **2002**, *23* (24), 4775–4785.

BM701176J